

Structural And Material Properties Of Ti-Si-N Nanocomposite Coatings

Y.V.Subba Rao^{a,b,c}, B.S.Gangadhara^b, E.Suresh Babu^c, K.S.Sumana^d

^a MRC-A.P.E.Research Lab, Materials Research Centre, Indian Institute of Science, Bangalore-12,India

^b Nanosys India, Bangalore-76, India,

^c A.P.E. Research S.r.l, Area Science Park, Basovizza, s.s. 14, Km 163,5 ,34149, Trieste,Italy,

^dDepartment of Physics, Maharani's Science College, Palace Road, Bangalore, India.

ABSTRACT

In this paper Ti-Si-N nanocomposite coatings were prepared by reactive magnetron sputtering on to different substrates at different power 50, 100, 150 and 200 watt at substrate temperature 400°. The presence of different phases like TiN, TiO₂ and SiN were confirmed by XPS analysis. From XRD analyses results, Ti-Si-N nanocomposite coatings are mainly composed of amorphous Si₃N₄ and TiN crystals with a grain size of 16 -30 nm. The Ti-Si-N coatings have somewhat mixed orientations (1 1 1), (2 2 0) and (2 0 0). The intensity of the (2 0 0) peak decreases with increasing in the content of power. The Topography and roughness parameter obtained using AFM and resistive properties using four probe method.

Keywords – Coatings, Nanocomposites, Sputtering, Si and Ti

1. INTRODUCTION

In recent years usage of hard coatings using Ti-Si-N have great importance for metal cutting and machine tool applications. It plays prominent role in industrial applications because of its high hardness, high temperature resistance, good wear and chemical stability [1-5]. Generally, techniques like Physical vapor deposition (PVD), Plasma assisted Chemical Vapour deposition are used for developing hard coatings on various substrates [6-8].

The aim of the present work is to study the effect of substrate Power on structure of Ti-Si-N thin films. The chemical structural, topography and resistivity parameters strongly dependent on the substrate power [9].

2. EXPERIMENTAL DETAILS

The 316L substrate surface was ground with SiC paper to remove the oxides and other contamination. The polished substrates were degreased alkali solution containing sodium hydroxide, followed by rinsing with triple distilled water. These substrates were subsequently dipped in 5 vol.-%H₂SO₄ solution for 1 min and thoroughly rinsed in distilled water.

Ti-Si-N nanocomposite coatings were deposited on different substrates by reactive DC magnetron sputtering deposition unit HIND HIVAC. The substrate temperature was 400°C High purity argon was fed into the vacuum chamber for the plasma generation. The substrates were etched for 5 min at a DC power of 50 W and an argon pressure of 10⁻⁶ Torr (1.33X 10⁻⁴Pa). High purity (99.99%) Ti and Si targets of 7.5 cm diameter was used as cathodes. The deposition parameters for Ti-Si-N sputtering are summarized in Table 2.1

2.1. Deposition parameters for Ti-Si-N nanocomposite coatings.

Table 2.1. Deposition parameters for Ti-Si-N

Objects	Specification
Target (2" Dia)	Ti & Si
Substrate	Glass, Si wafer, 316L Stainless steel
Target to substrate distance	60 mm
Ultimate vacuum	1 x 10 ⁻⁶ m bar
Operating vacuum	2 x 10 ⁻³ m bar
Sputtering gas (Ar: N ₂)	2: 1
Power	50, 100, 150, 200 W
Substrate temperature	400 °C

Ti-Si-N nanocomposite films chemical nature was obtained by X-ray photoelectron spectroscopy (XPS) using Multilab 2000. The structural confirmation was obtained by X-Ray Diffraction studies carried out using Bruker X-ray diffractometer by using Cu K α radiation ($\lambda=1.5406$ Å). The topography and roughness of the films was analysed atomic force microscope (Model: A.P.E.Research A-100) and resistivity of films calculated from the four Probe method.

3. RESULTS AND DISCUSSION

3.1. X-ray photoelectron spectroscopy analysis

XPS survey spectra of the Ti-Si-N nanocomposite coatings shown in Fig.5.1a. The coatings exhibit the characteristic Ti2p, Si2p, N1s, O1s and C1s peaks at the corresponding binding energies 458.7, 101.5, 396.3, 531.7 and 283.8 eV respectively. The high resolution spectra of Ti2p showed (Fig.5.1b) the presence of oxide (TiO₂) and

nitride (TiN) phases in the surface at the corresponding binding energies 465.1 and 459.2 eV. The binding energy of Si2p at 102.5 eV (Fig.5.1c) corresponds to stoichiometric Si₃N₄. A peak on 396.4 eV shows the formation of TiN phase (Fig.5.1d). The C 1s spectra of the films in Fig. 5.1e show a typical characteristic of C-C bond with binding energy around 284.9 eV [8,10]

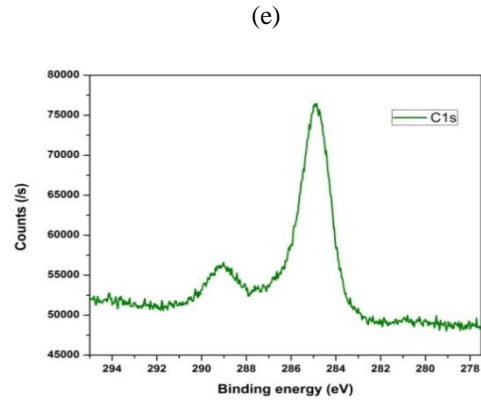
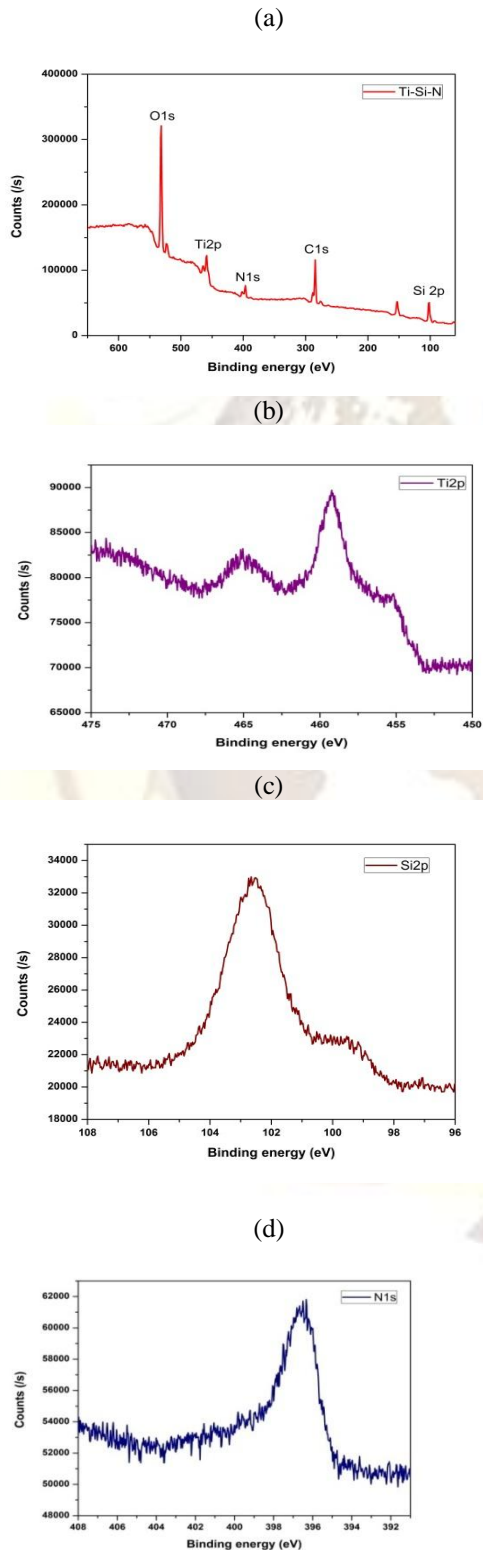


Fig.3.1.Survey spectra of the Ti-Si-N coatings (a) Survey, (b) Ti2p (c) Si2p (d) N1s (e) C1s.

3.2. X-Ray Diffraction

X-ray diffraction pattern of Ti-Si-N nanocomposite coatings deposited onto glass substrate at different powers is show in Fig.5.2.

The pattern shows only diffraction peaks due to crystalline TiN are observed, with no indication of the presence of crystalline Si₃N₄ phases, suggesting that Si is present in amorphous state at deposited power of 50 W. The observed d values are in good agreement with the standard values with JCPDS card no 087-0633 for TiN coatings. XRD patterns revealed the presence of only one phase that can be assigned to the cubic B1 NaCl structure, typical for TiN and the peaks corresponding to (111), (200) and (220) planes were observed.

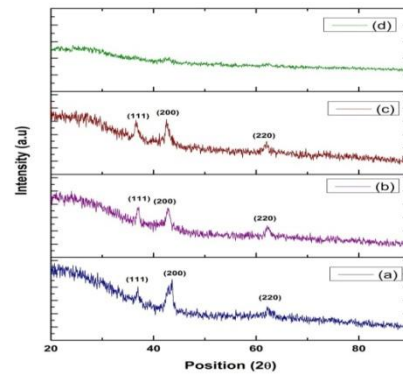


Fig.3.2 XRD patterns for Ti-Si-N coatings (a) 50 watt (b) 100 watt (c) 150 watt (d) 200 watt

The X-ray diffraction pattern of Ti-Si-N films which shows only diffraction peaks with a strongly TiN (2 0 0) preferred orientation at low power. It is probably a solid solution (Ti, Si) N by a substitution of Si for Ti in TiN lattice, because the ionic radius of Si⁴⁺ ion (0.041nm) is smaller than that of Ti³⁺ (0.075 nm) ion. The Ti-Si-N coatings have somewhat mixed orientations (1 1 1), (2 2 0) and (2 0 0). The intensity of the (2 0 0) peak decreases with increasing in the content of power[8]

Table 3.2 (a), (b), (c) and (d) shows calculation of the grain size, dislocation density, lattice parameter, strain, texture coefficient and micro strain. The grain size can be calculated from XRD pattern, using the formula.

$$\text{Grain size: } D = \frac{0.9\lambda}{\beta \cos \theta} \quad (5.1)$$

Where, λ → wave length of x – ray (nm)
 β → Full width half maximum (mm)
 θ → Position

Increasing the substrate power, grain size decreases whereas strain was found to increase. The larger grain size of the film grown at 50 W is also an evidence of its high compaction (decreasing the grain boundaries) confirmed by the highest intensity of the diffraction peak for this temperature.

3.3. Morphological studies

The surface topography of the Ti-Si-N coatings was studied using Atomic force microscopy (AFM). The basic study comprised 2D and 3D representations for a scanned area of 2X 2 μm , which are shown in Fig 3.3. The roughness value, estimated from these images was 5.6 nm, which shows that the films were very smooth in nature^[7]

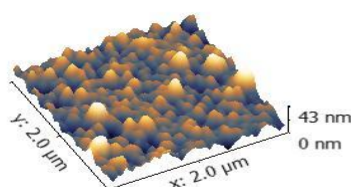
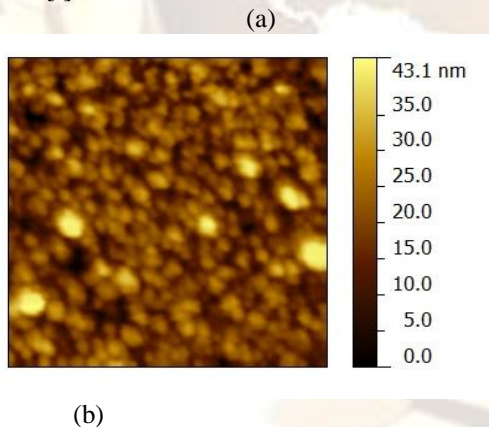


Fig .3.3. AFM Images of Ti-Si-N (a)2D Image

(b)3D Image

3.4. Electrical studies

Electrical resistivity measurements of Ti-Si-N coatings on glass substrates were performed using four-probe method at room temperature. In this technique four probes are placed on a flat surface of the substrates. Current is passed through the two outer electrodes and the floating potential is measured across the inner pair. A nominal value of probe spacing, which has been found satisfactory, is an equal distance of 1.5 nm between adjacent probes. Resistivity can be calculated from the formulae

$$\rho = 4.532 \times (V/I) \times t \quad \text{-----(Equation 3.4)}$$

Where, V- measured voltage
 I - current passed
 t – thickness of the coating

Power (watt)	Resistivity ($\mu\text{ohm-cm}$)			
	38°C	50°C	100°C	150°C
50	46.66	44.4	43.5	41.9
100	16.6	16.74	16.53	16.24
150	9.5	9.59	9.73	9.73
200	47.2	47.0	46.2	45.4

Table.3.3. The electrical resistivity of the Ti-Si-N coatings for various substrate temperatures. Resistivity values of Ti-Si-N hard coatings in the range of 9-47 $\mu\text{ohm-cm}$ are given in Table.3.3. It shows that these films have low electrical resistivity. When the power is increased the electrical resistivity was found to decrease. While at a higher Si concentration the resistivity increases (Fig.3.4).

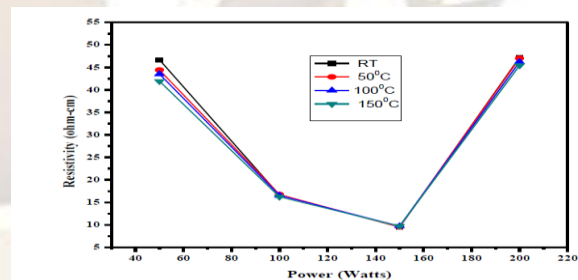


Fig.3.4 Resistivity measurements various temperatures.

I. CONCLUSION

Ti-Si-N nanocomposite coatings were prepared by reactive magnetron sputtering on to different substrates at different power. The presence of different phases like TiN, TiO₂ and SiN were confirmed by XPS analysis. From XRD analyses results, Ti-Si-N nanocomposite coatings are mainly composed of amorphous Si₃N₄ and TiN crystals with a grain size of several nanometers. The Ti-Si-N coatings have somewhat mixed orientations (1 1 1), (2 2 0) and (2 0 0). The intensity of the (2 0 0)

peak decreases with increasing in the content of power. AFM analysis indicated that the coatings were regular with smooth structure . The Ti-Si-N shows low electrical resistivity coatings in the range of 9-47 $\mu\text{ohm-cm}$.

REFERENCES

- [1] R.F. Bunshah (Ed.), *Handbook of Hard Coatings; Deposition Technologies, Properties and Applications*, (Noyes publications, Park ridge, New Jersey, USA, 2001).
- [2] Veprek, S. Reiprich, Mechanical properties of superhard nanocomposites, *Thin Solid Films* 268 (1995) 64.
- [3] C.W. Zou, H.J. Wang, M. Li, Y.F. Yu, C.S. Liu, L.P. Guo, D.J. Fu, Characterization and properties of TiN-containing amorphous Ti-Si-N nanocomposite coatings prepared by arc assisted middle frequency magnetron sputtering, *Vacuum* 84 (2010) 817–822
- [4] S. Guruvenket , D. Li , J.E. Klemberg-Sapieha , L. Martinu, J. Szpunar, Mechanical and tribological properties of duplex treated TiN, nc-TiN/a-SiNx and nc-TiCN/a-SiCN coatings deposited on 410 low alloy stainless steel, *Surface & Coatings Technology* 203 (2009) 2905–2911
- [5] K. Holmberg, A. Matthews, *Techniques and Applications in Surface Engineering, Coatings Tribology: Properties*, Elsevier, New York, 1994
- [6] J. Bonse, P. Rudolph, J. Kruger, S. Baudach and W. Kautek, Ultrashort pulse laser ablation of polycarbonate and polymethylmethacrylate *Appl. Surf. Sci.*154/155, (2000), 659.
- [7] Vipin chawla, RJayaganthan, and Ramesh Chandra, Microstructural characteristics and mechanical properties of magnetron sputtered nanocrystalline TiN films on glass substrate, *Bull. Mater. Sci.*, Vol. 32, No. 2, April 2009, pp. 117–123.
- [8] M. Nose , Y. Deguchi, T. Mae, E. Honbo, T. Nagae, K. Nogi, Influence of sputtering conditions on the structure and properties of Ti-Si-N thin films prepared by r.f.-reactive sputtering, *Surface and Coatings Technology* 174 –175 (2003) 261–265
- [9] Albano cavalerio, Jeff Th. M. De Hosson, *Nanostructured coatings*, (p183, Springer ,2006).
- [10] Hui-Wen Chang , Ping-Kang Huang , Jien-Wei Yeh ,Andrew Davison, Chun-Huei Tsau, Chih-Chao Yang, Influence of substrate bias, deposition temperature and post-deposition annealing on the structure and properties of multi-principal-component(AlCrMoSiTi)N coatings, *Surface & Coatings Technology* 202 (2008) 3360–3366
- [12] Ping Zhang , Zhihai Cai, Wanquan Xiong, Influence of Si content and growth condition on the microstructure and mechanical properties of Ti-Si-N nanocomposite films, *Surface & Coatings Technology* 201 (2007) 6819–6823